bands and the SCN5A-negative probands. *Am J Cardiol* 2007; **100:** 649–655.
8. Meregalli PG, Wilde AA, Tan HL. Pathophysiological mechanisms of Brugada syndrome: Depolarization disorder, repolarization disorder, or more? *Cardiovasc Res* 2005; **67:** 367–378.
9. Smits JP, Eckardt L, Probst V, Bezzina CR, Schott JJ, Remme CA, et al. Genotype-phenotype relationship in Brugada syndrome: Electrocardiographic features differentiate SCN5A-related patients from non-SCN5A-related patients. *J Am Coll Cardiol* 2002; **40:** 350–356.
10. Probst V, Allouis M, Sacher F, Pattier S, Babuty D, Mabo P, et al. Progressive cardiac conduction defect is the prevailing phenotype in carriers of a Brugada syndrome SCN5A mutation. *J Cardiovasc Electrophysiol* 2006; **17:** 270–275.
11. Makiyama T, Akao M, Tsuji K, Doi T, Ohno S, Takenaka K, et al. High risk for bradyarrhythmic complications in patients with Brugada syndrome caused by SCN5A gene mutations. *J Am Coll Cardiol* 2005; **46:** 2100–2106.
12. Shimizu N, Iwamoto M, Nakano Y, Sumita S, Ishikawa T, Hokosaki T, et al. Long-term electrocardiographic follow-up from childhood of an adult patient with Brugada syndrome associated with sick sinus syndrome. *Circ J* 2009; **73:** 575–579.
13. Makiyama T, Akao M, Haruna Y, Tsuji K, Doi T, Ohno S, et al. Mutation analysis of the glycerol-3 phosphate dehydrogenase-1 like (GPD1L) gene in Japanese patients with Brugada syndrome. *Circ J* 2008; **72:** 1705–1706.
14. Shimizu W. Clinical impact of genetic studies in lethal inherited cardiac arrhythmias. *Circ J* 2008; **72:** 1926–1936.
15. Gehi AK, Duong TD, Metz LD, Gomes JA, Mehta D. Risk stratification of individuals with the Brugada electrocardiogram: A meta-analysis. *J Cardiovasc Electrophysiol* 2006; **17:** 577–583.
16. Junttila MJ, Brugada P, Hong K, Lizotte E, DE Zutter M, Sarkozy A, et al. Differences in 12-lead electrocardiogram between symptomatic and asymptomatic Brugada syndrome patients. *J Cardiovasc Electrophysiol* 2008; **19:** 380–383.
17. Morita H, Morita ST, Nagase S, Banba K, Nishii N, Tani Y, et al. Ventricular arrhythmia induced by sodium channel blocker in patients with Brugada syndrome. *J Am Coll Cardiol* 2003; **42:** 1624–1631.
18. Morita H, Fukushima-Kusano K, Nagase S, Takenaka-Morita S, Nishii N, Kakishita M, et al. Site-specific arrhythmogenesis in patients with Brugada syndrome. *J Cardiovasc Electrophysiol* 2003; **14:** 373–379.
19. Nagase S, Kusano KF, Morita H, Fujimoto Y, Kakishita M, Nakamura K, et al. Epicardial electrogram of the right ventricular outflow tract in patients with the Brugada syndrome: Using the epicardial lead. *J Am Coll Cardiol* 2002; **39:** 1992–1995.
20. Wang Q, Shen J, Splawski I, Atkinson D, Li Z, Robinson JL, et al. SCN5A mutations associated with an inherited cardiac arrhythmia, long QT syndrome. *Cell* 1995; **80:** 805–811.
21. Tada T, Kusano KF, Nagase S, Banba K, Miura D, Nishii N, et al. Clinical significance of macroscopic T-wave alternans after sodium channel blocker administration in patients with Brugada syndrome. *J Cardiovasc Electrophysiol* 2008; **19:** 56–61.
22. Kusano KF, Taniyama M, Nakamura K, Miura D, Banba K, Nagase S, et al. Atrial fibrillation in patients with Brugada syndrome relationships of gene mutation, electrophysiology, and clinical backgrounds. *J Am Coll Cardiol* 2008; **51:** 1169–1175.
23. Chen Q, Kirsch GE, Zhang D, Brugada R, Brugada J, Brugada P, et al. Genetic basis and molecular mechanism for idiopathic ventricular fibrillation. *Nature* 1998; **392:** 293–296.
24. Priori SG, Napolitano C, Gasparini M, Pappone C, Della Bella P, Giordano U, et al. Natural history of Brugada syndrome: Insights for risk stratification and management. *Circulation* 2002; **105:** 1342–1347.
25. Priori SG, Napolitano C, Gasparini M, Pappone C, Della Bella P, Brignole M, et al. Clinical and genetic heterogeneity of right bundle branch block and ST-segment elevation syndrome: A prospective evaluation of 52 families. *Circulation* 2000; **102:** 2509–2515.
26. Hu D, Viskin S, Oliva A, Carrier T, Cordeiro JM, Barajas-Martinez H, et al. Novel mutation in the SCN5A gene associated with arrhythmic storm development during acute myocardial infarction. *Heart Rhythm* 2007; **4:** 1072–1080.
27. Aiba T, Shimizu W, Hidaka I, Uemura K, Noda T, Zheng C, et al. Cellular basis for trigger and maintenance of ventricular fibrillation in the Brugada syndrome model: High-resolution optical mapping study. *J Am Coll Cardiol* 2006; **47:** 2074–2085.
28. Ikeda T, Takami M, Sugi K, Mizusawa Y, Sakurada H, Yoshino H. Noninvasive risk stratification of subjects with a Brugada-type electrocardiogram and no history of cardiac arrest. *Ann Noninvasive Electrocardiol* 2005; **10:** 396–403.

Circulation
JOURNAL OF THE AMERICAN HEART ASSOCIATION

American Heart Association®
Learn and Live℠

Three-Dimensional Structure of Pulmonary Capillary Vessels in Patients With Pulmonary Hypertension

Aya Miura, Kazufumi Nakamura, Kengo F. Kusano, Hiromi Matsubara, Aiko Ogawa, Satoshi Akagi, Takahiro Oto, Takuro Murakami, Aiji Ohtsuka, Chikao Yutani, Tohru Ohe and Hiroshi Ito

Circulation 2010;121;2151-2153
DOI: 10.1161/CIR.0b013e3181e037c1
Circulation is published by the American Heart Association. 7272 Greenville Avenue, Dallas, TX 72514
Copyright © 2010 American Heart Association. All rights reserved. Print ISSN: 0009-7322. Online ISSN: 1524-4539

The online version of this article, along with updated information and services, is located on the World Wide Web at:
http://circ.ahajournals.org/cgi/content/full/121/19/2151

Subscriptions: Information about subscribing to Circulation is online at
http://circ.ahajournals.org/subscriptions/

Permissions: Permissions & Rights Desk, Lippincott Williams & Wilkins, a division of Wolters Kluwer Health, 351 West Camden Street, Baltimore, MD 21202-2436. Phone: 410-528-4050. Fax: 410-528-8550. E-mail:
journalpermissions@lww.com

Reprints: Information about reprints can be found online at
http://www.lww.com/reprints

Downloaded from circ.ahajournals.org at OKA-DAI FUZOKU TOSHOKAN SHIKAT on May 2, 2011

Three-Dimensional Structure of Pulmonary Capillary Vessels in Patients With Pulmonary Hypertension

Aya Miura, MSc*; Kazufumi Nakamura, MD, PhD*; Kengo F. Kusano, MD, PhD; Hiromi Matsubara, MD, PhD; Aiko Ogawa, MD, PhD; Satoshi Akagi, MD, PhD; Takahiro Oto, MD, PhD; Takuro Murakami, MD, PhD; Aiji Ohtsuka, MD, PhD; Chikao Yutani, MD, PhD; Tohru Ohe, MD, PhD; Hiroshi Ito, MD, PhD

Pulmonary arterial hypertension, pulmonary veno-occlusive disease, and pulmonary capillary hemangiomatosis are included in the same group (group 1) of clinical classification of pulmonary hypertension.[1] Histological changes in the small pulmonary arteries (ie, intimal fibrosis and medial hypertrophy) are similar in these 3 diseases, and clinical presentations of the 3 diseases are often indistinguishable.[1] However, it is estimated that the hemodynamics of capillary vessels are quite different in each disease. The hemodynamics of capillary vessels (ie, capillary occlusion) play an important role in cardiovascular diseases.[2] Thus, clarification of the differences in the hemodynamics is essential to understand the pathophysiology of these 3 diseases.

We obtained lung segments from patients with pulmonary hypertension who underwent living-donor lung transplantation and from patients with bronchogenic carcinoma who underwent lobectomy as described previously.[3] All experiments were performed after approval was obtained from the Human Ethics Committee of Okayama University, and written informed consent was obtained from all patients before the procedure. We succeeded in visualization of the 3-dimensional structure of the pulmonary capillary in patients with pulmonary arterial hypertension, pulmonary veno-occlusive disease, and pulmonary capillary hemangiomatosis using scanning electron microscopy of blood vascular casts.[4]

A 42-year-old man underwent lobectomy for bronchogenic carcinoma. Figure 1A shows hematoxylin-eosin staining of a normal small pulmonary artery. Blood vascular architecture in the most distal area from the carcinoma in the resected lobe shows a normal capillary network around the alveolus of the lung (Figure 1B).

A 20-year-old man underwent lung transplantation for idiopathic pulmonary arterial hypertension. The blood vascular architecture resembled dead branches. The small vessels were severely stenosed and were often occluded (Figure 2A), and the capillary was deficient (Figure 2B).

A 27-year-old man underwent lung transplantation for pulmonary veno-occlusive disease. The small pulmonary veins were stenosed (Figure 3A), and capillary vessels were swollen compared with a normal capillary (Figure 3B).

A 14-year-old boy underwent lung transplantation for pulmonary capillary hemangiomatosis. A proliferation of capillaries was seen (Figure 4A), and the capillary vessels resembled a tumorous cluster (Figure 4B).

Scanning electron microscopic study of blood vascular casts revealed the differences in the 3 diseases. Pulmonary arterial hypertension was characterized by a deficient capillary network, pulmonary veno-occlusive disease by swollen capillary vessels, and pulmonary capillary hemangiomatosis by a tumorlike outgrowth of capillaries. To the best of our knowledge, this is the first report on differences in the 3-dimensional structure of capillary vessels in normal controls, pulmonary arterial hypertension, pulmonary veno-occlusive disease, and pulmonary capillary hemangiomatosis using scanning electron microscopy of blood vascular casts. These findings provide an insight into the basic mechanism responsible for pulmonary hypertension.

Sources of Funding

This work was supported by the Research Grant for Cardiovascular Diseases (19–9) from the Ministry of Health, Labour and Welfare, Japan.

Disclosures

None.

References

1. Simonneau G, Robbins IM, Beghetti M, Channick RN, Delcroix M, Denton CP, Elliott CG, Gaine SP, Gladwin MT, Jing ZC, Krowka MJ, Langleben D, Nakanishi N, Souza R. Updated clinical classification of pulmonary hypertension. *J Am Coll Cardiol*. 2009;54:S43–S54.
2. Ito H. No-reflow phenomenon and prognosis in patients with acute myocardial infarction. *Nat Clin Pract Cardiovasc Med*. 2006;3:499–506.
3. Ogawa A, Nakamura K, Matsubara H, Fujio H, Ikeda T, Kobayashi K, Miyazaki I, Asanuma M, Miyaji K, Miura D, Kusano KF, Date H, Ohe T. Prednisolone inhibits proliferation of cultured pulmonary artery smooth muscle cells of patients with idiopathic pulmonary arterial hypertension. *Circulation*. 2005;112:1806–1812.
4. Murakami T. Application of the scanning electron microscope to the study of the fine distribution of the blood vessels. *Arch Histol Jpn*. 1971;32:445–454.

From the Department of Cardiovascular Medicine (A.M., K.N., K.F.K., A. Ogawa, S.A., T. Ohe, H.I.), Department of Cancer and Thoracic Surgery (T. Oto), and Department of Human Morphology (T.M., A. Ohtsuka), Okayama University Graduate School of Medicine, Dentistry, and Pharmaceutical Sciences; Division of Cardiology, National Hospital Organization, Okayama Medical Center (H.M.); and Department of Life Science (C.Y.), Okayama University of Science, Okayama, Japan.

*The first 2 authors contributed equally to this work.

Correspondence to Kazufumi Nakamura, MD, PhD, Department of Cardiovascular Medicine, Okayama University Graduate School of Medicine, Dentistry, and Pharmaceutical Sciences, 2-5-1 Shikata-cho, Okayama 700-8558, Japan. E-mail ichibun@cc.okayama-u.ac.jp

(*Circulation*. 2010;121:2151-2153.)

© 2010 American Heart Association, Inc.

Circulation is available at http://circ.ahajournals.org

DOI: 10.1161/CIR.0b013e3181e037c1

Downloaded from circ.ahajournals.org at OKA-DAIGAKU TOSHOKAN SHIKAT on May 2, 2011

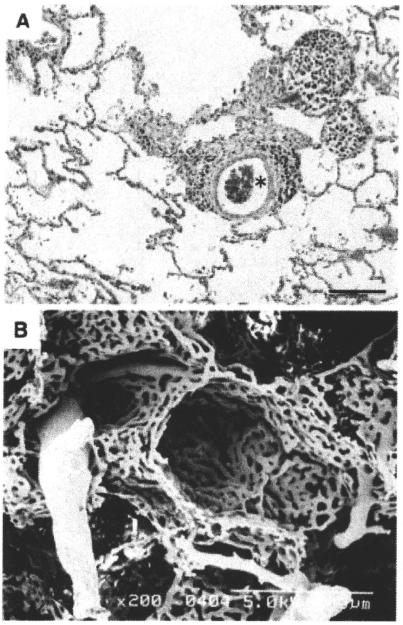

Figure 1. Images of normal control microvessels. A, Hematoxylin-eosin staining of a small pulmonary artery (*). Bar=200 μm. B, Scanning electron micrograph of blood vascular casts. Bar=200 μm.

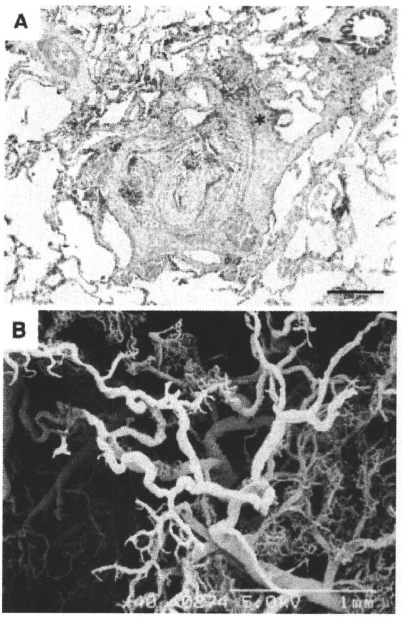

Figure 2. Images of microvessels from a patient with pulmonary arterial hypertension. A, Hematoxylin-eosin staining of small pulmonary arteries (*). Bar=200 μm. B, Scanning electron micrograph of blood vascular casts. A deficient capillary network is seen. Bar=1 mm.

Downloaded from circ.ahajournals.org at OKA-DAI FUZOKU TOSHOKAN SHIKAT on May 2, 2011

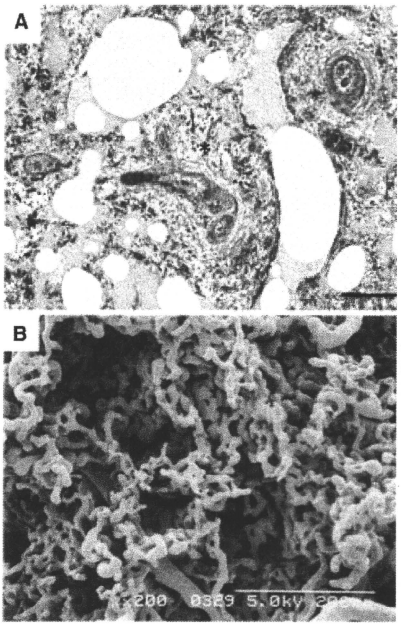

Figure 3. Images of microvessels from a patient with pulmonary veno-occlusive disease. A, Masson's trichrome staining of a small pulmonary vein (*). Bar=200 μm. B, Scanning electron micrograph of blood vascular casts. Swollen capillary vessels are seen. Bar=200 μm.

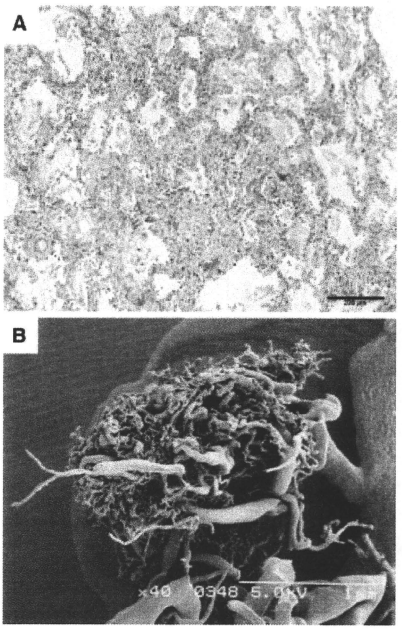

Figure 4. Images of microvessels from pulmonary capillary hemangiomatosis. A, Hematoxylin-eosin staining of small pulmonary vessels. Bar=200 μm. B, Scanning electron micrograph of blood vascular casts. Tumorlike outgrowth of capillary vessels is seen. Bar=1 mm.

Downloaded from circ.ahajournals.org at OKA-DAI FUZOKU TOSHOKAN SHIKAT on May 2, 2011

ELSEVIER

Cardiovascular Pathology 20 (2011) e37–e42

CARDIOVASCULAR PATHOLOGY

Original Article

Elevated oxidative stress is associated with ventricular fibrillation episodes in patients with Brugada-type electrocardiogram without SCN5A mutation

Masamichi Tanaka[a], Kazufumi Nakamura[a,*], Kengo Fukushima Kusano[a], Hiroshi Morita[a], Keiko Ohta-Ogo[a], Daiji Miura[a], Aya Miura[a], Koji Nakagawa[a], Takeshi Tada[a], Masato Murakami[a], Nobuhiro Nishii[a], Satoshi Nagase[a], Yoshiki Hata[a], Kunihisa Kohno[a], Mamoru Ouchida[b], Kenji Shimizu[b], Chikao Yutani[c], Tohru Ohe[a,d], Hiroshi Ito[a]

[a]*Department of Cardiovascular Medicine, Okayama University Graduate School of Medicine, Dentistry and Pharmaceutical Sciences, Okayama, Japan*
[b]*Department of Molecular Genetics, Okayama University Graduate School of Medicine, Dentistry and Pharmaceutical Sciences, Okayama, Japan*
[c]*Department of Life Science, Okayama University of Life Science, Okayama, Japan*
[d]*Department of Cardiology, Cardiovascular Center, Sakakibara Hospital, Okayama, Japan*

Received 21 October 2009; received in revised form 19 January 2010; accepted 6 February 2010

Abstract

Background: Brugada syndrome is a disease known to cause ventricular fibrillation with a structurally normal heart and is linked to SCN5A gene mutation. However, the mechanism by which ventricular fibrillation develops in cases of Brugada-type electrocardiogram without SCN5A mutation has remained unclear. Recently, oxidative stress has been implicated in the pathophysiology of cardiac arrhythmia. We also investigated oxidative stress levels in the myocardia of patients with Brugada-type electrocardiogram. **Methods:** Endomyocardial biopsy samples were obtained from 68 patients with Brugada-type electrocardiogram (66 males and two females). We performed histological and immunohistochemical analyses for CD45, CD68, and 4-hydroxy-2-nonenal-modified protein, which is a major lipid peroxidation product. **Results:** SCN5A mutation was detected in 14 patients. Ventricular fibrillation was documented in three patients with SCN5A mutation and in 11 without SCN5A mutation. In patients with SCN5A mutation, 4-hydroxy-2-nonenal-modified protein-positive area was not significantly different between the documented ventricular fibrillation (VF) group (VF+ group) and the group without documented VF (VF− group). However, in patients without SCN5A, the area was significantly larger in the VF+ group than that in the VF− group ($P<.05$). All other parameters (fibrosis area, CD45, and CD68) were not different between the VF+ and VF− group in both SCN5A+ and SCN5A− patients. **Conclusion:** Oxidative stress is elevated in the myocardium of patients with Brugada-type electrocardiogram who have VF episodes and do not have SCN5A gene mutations. Oxidative stress may be associated with the occurrence of VF in patients with Brugada-type electrocardiogram without SCN5A mutation. © 2011 Elsevier Inc. All rights reserved.

Keywords: Oxidative stress; Ventricular fibrillation; Brugada syndrome

1. Introduction

Brugada syndrome (BS) is a disease characterized by ST-segment elevation in right precordial leads and episodes of ventricular fibrillation (VF) in the absence of structural heart disease [1]. About 20% of BS cases have been linked to mutations in the SCN5A gene, the gene encoding the alpha subunit of the cardiac sodium channel [2,3]. Functional analysis employing expression systems has revealed that mutations in SCN5A resulted in "loss of function" of I_{Na}, which reduces the inward sodium current, induces conduction delay, and predisposes the substrate for reentry. Other

This work was supported in part by a Grant-in-Aid for Exploratory Research from the Ministry of Education, Culture, Sports, Science and Technology (No. 19659205), Japan, and in part by a Health Sciences Research grant (H18—Research on Human Genome—002) from the Ministry of Health, Labor and Welfare, Japan.

* Corresponding author. Department of Cardiovascular Medicine, Okayama University Graduate School of Medicine Dentistry and Pharmaceutical Sciences, 2-5-1 Shikata-cho, Kita-ku, Okayama 700-8558, Japan. Tel.: +81 86 235 7351; fax: +81 86 235 7353.

E-mail addresses: ichibun@cc.okayama-u.ac.jp, ichibun@yahoo.co.jp (K. Nakamura).

1054-8807/10/$ – see front matter © 2011 Elsevier Inc. All rights reserved.
doi:10.1016/j.carpath.2010.02.002

gene mutations such as CACNA1c [4], CACNB2b [4], GPD1-L [5], SCN1B [6], and KCNE3 [7] have also been reported. However, cases with such mutations are not frequent and the prevalence of those mutations is not clear [8]. Recently, Frustaci et al. [9] reported that lymphocytic myocarditis was observed in patients with Brugada-type electrocardiogram (ECG) who did not have SCN5A gene mutations, but the association with histological findings and occurrence of ventricular fibrillation (VF) has not been fully elucidated. Thus, the mechanism by which VF develops in cases of Brugada-type ECG without SCN5A mutation has remained unclear.

Recently, oxidative stress has been implicated in the pathophysiology of cardiac arrhythmia. Hydrogen peroxide (H_2O_2) decreases SCN5A transcription and current [10]. E2-isoketal, a highly reactive product of lipid peroxidation, potentiates inactivation of cardiac Na^+ channels [11]. Reactive oxygen species (ROS) contribute to cardiac sympathovagal imbalance in cardiomyocytes [12]. We also investigated oxidative stress levels, assessed by expression levels of 4-hydroxy-2-nonenal (HNE)-modified protein, a reliable marker of lipid peroxidation [13,14], in the myocardia of patients with Brugada-type ECG and investigated the association between VF events and oxidative stress levels in the myocardia of patients with Brugada-type ECG with and without mutation in the SCN5A gene.

2. Methods

2.1. Subjects

In the period from June 1998 to June 2008, we performed electrophysiological study and endomyocardial biopsy in 68 consecutive patients with Brugada-type electrocardiogram (ECG) (66 males and two females; mean age, 49.0 years). Brugada-type ECG was defined as coved ST-segment elevation (>0.2 mV) followed by a negative T-wave in more than one right precordial lead (V1 to V3) or third intercostal leads (V1 to V2) in the presence or absence of a sodium channel blocker (Fig. 1). Routine examinations, including cardiac echocardiography, coronary angiography, and right and left ventriculography, showed no evidence of structural heart disease in any of the patients. We examined the clinical characteristics of patients, including age, sex, spontaneous VF occurrence, history of syncope, family history of sudden death, and SCN5A mutation.

2.2. Cardiac catheterization, endomyocardial biopsy, and electrophysiological study

After providing written informed consent, all patients underwent cardiac catheterization, coronary angiography, right and left ventricular angiography, and endomyocardial

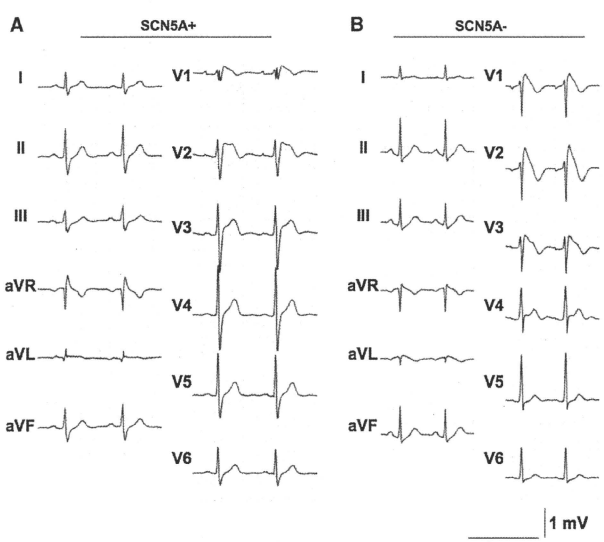

Fig. 1. Representative ECGs of patients with or without SCN5A mutation. (A) ECG of a patient with SCN5A mutation (SCN5A+), R282H (47 years old, male). (B) ECG of a patient without SCN5A mutation (SCN5A−) (42 years old, male).

biopsy. Endomyocardial biopsy samples (three or four per patient for histology) were obtained from the right ventricular (RV) side of the septum of all patients by the internal jugular approach.

The electrophysiological study was performed in all patients as reported previously [15,16]. The risks of the electrophysiological study were explained to each patient, and written informed consent was obtained from all patients. Induction of ventricular arrhythmia was initially attempted without the use of any antiarrhythmic drugs. The criterion for the induction of ventricular arrhythmia was induction of VF by programmed electrical stimulation from the RV apex, RV outflow tract, or left ventricle with a maximum of two extrastimuli at two cycle lengths.

2.3. Histology and immunohistochemistry

Endomyocardial biopsy samples were fixed in 10% formalin and embedded in paraffin. For histology, 5-μm-thick sections were cut and stained with hematoxylin and eosin and Masson's trichrome stain and examined by light microscopy.

Immunoenzymatic staining was performed using a DAKO LSAB System (Dako) according to the manufacturer's instructions, as previously described [13,14,17]. Briefly, the heart sections embedded in paraffin were preincubated with 1.5% hydrogen peroxide and normal BSA to block nonspecific reactions. CD45RO (1:100) and CD68 (1:50) antibodies (both from Dako) for the characterization of inflammatory infiltrate, and mouse monoclonal anti-HNE-modified protein antibody (1:50 dilution, NOF Medical Department) for assessment of oxidative stress were added. After incubation at 4°C overnight, the sections were incubated with biotinylated anti-mouse immunoglobulin for 20 min and subsequently with horseradish peroxidase-labeled streptavidin solution for 20 min. The slides were rinsed in cold Tris-buffered saline after each step of incubation. Peroxidase activity was visualized with diaminobenzidine (DAB) tetrahydrochloride solution.

2.4. Semiquantitative analysis of stained samples

Digital images of stained sections were taken with a Fujix Digital Camera HC-300/OL mounted on an Olympus BH-2 microscope. Color images from five randomly selected separate high-power fields (×200) in three or four sections per patient were obtained. Staining was analyzed using WinROOF Image software (Mitani Corp.) and assessed by using the following equation: stained area (%)=100×stained area (cm^2)/total sample size (cm^2).

CD45RO- and CD68-positive cells were counted by the following equation: inflammatory cell infiltration=number of CD45RO- or CD68-positive cells (n)/total sample size (cm^2).

2.5. Genetic analysis

Genetic analysis was performed in compliance with the guidelines for human genome studies of the Ethics Committee of Okayama University. Informed consent was obtained from all subjects. Genomic DNA was extracted from peripheral blood leukocytes by using a DNA extraction kit (Gentra, Minneapolis, MN, USA) and was stored at −30°C until use.

Twenty-seven exons of the SCN5A gene were amplified with previously reported intronic primers [18]. SCN5A gene exon 1 is a noncoding region, and we did not analyze this region in this study. Exons 6, 17–1 sense, 21, and 25 were not able to be sufficiently amplified by the primers, and we therefore designed the following intronic primers as previously described [19,20]. The primers used in this study are as follows: 5′-GTT ATC CCA GGT AAG ATG CCC-3′ (sense) and 5′-TGG TGA CAG GCA CAT TCG AAG-3′ (anti-sense) for exon 6; 5′-AAG CCT CGG AGC TGT TTG TCA CA-3′ (sense) for exon 17–1; 5′-TGC CTG GTG CAG GGT GGA AT-3′ (sense) and 5′-ACT CAG ACT TAC GTC CTC CTT C-3′ (anti-sense) for exon 21; 5′-TCT TTC CCA CAG AAT GGA CAC C-3′ (sense) and 5′-AAG GTG AGA TGG GAC CTG GAG-3′ (anti-sense) for exon 25. PCR was performed in a 20-μl reaction volume containing 50 ng of genomic DNA, 20 pmol of each primer, 0.8 mM dNTPs, 1× reaction buffer, 1.5 mM $MgCl_2$, and 0.7 U of AmpliTaq Gold DNA polymerase (Applied Biosystems, Foster City, CA, USA) or TAKARA Taq (Takara Bio, Inc., Otsu, Shiga, Japan). All PCR products were treated with exonuclease I (New England BioLabs, Ipswich, MA, USA) and shrimp alkaline phosphatase (USB Corporation, Cleveland, OH, USA), reacted with a Big Dye Terminator v. 1.1 cycle sequencing kit (Applied Biosystems) and analyzed on an ABI PRISM3130 XL sequencer (Applied Biosystems). The mutations were confirmed four times by independent PCR amplification and sequencing.

2.6. Statistical analysis

Data are all expressed as means±S.D. Intergroup comparison was done by Fisher's Exact Probability Test, and difference in mean values was tested by Student's t test,

Table 1
Patients' characteristics

Number	68
Age, years	49.0±11.6
Male/female	66/2
Family history of SCD (%)	19 (16.1)
Syncope (%)	12 (27.9)
ICD Implantation (%)	22 (32.8)
SCN5A Mutation (%)	14 (20.6)
Documented VF (%)	14 (20.6)
SCN5A mutation+ (%)	3 (4.4)
SCN5A mutation− (%)	11 (16.2)

Data are mean±S.D.
SCD: Sudden cardiac death; ICD: implanted cardioverter defibrillator; VF: ventricular fibrillation.

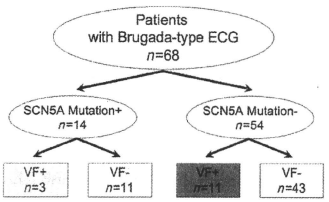

Fig. 2. Study profile.

at a critical level of 5% or lower. All data were analyzed using SPSS software (version 11.0.1).

3. Results

3.1. Patients' characteristics

Clinical characteristics of all patients with Brugada-type ECG are shown in Table 1. SCN5A mutation was detected in 14 patients. VF was documented in three patients with SCN5A mutation and in 11 patients without SCN5A mutation (Table 1 and Fig. 2).

Eleven patients (two patients with SCN5A mutation and nine patients without mutation) had histories of spontaneous VF that was converted to sinus rhythm by an external defibrillator before admission. In the other three patients (one patient with SCN5A mutation and two patients without the mutation), spontaneous VF occurred de novo after discharge from our hospital and was terminated by implantable cardioverter defibrillator therapy. There was no death in any of the patients.

3.2. Histology and immunohistochemistry

HNE-modified protein-positive area in patients with documented VF (VF+ group) was larger than that in patients without documented VF (VF− group) (VF+ group: 16.3 ±10.5% vs. VF− group: 9.3±5.7%, $P<.05$) (Fig. 3A). There were no significant differences in area of fibrosis and number of CD45RO- and CD68-positive cells between the VF+ and VF− groups.

We also checked those parameters in patients with and without SCN5A mutation. HNE-modified protein-positive areas were not significantly different in the SCN5A+ and SCN5A− patients (SCN5A+ group: 13.3±7.6% vs. SCN5A − group: 10.1±7.3%, P=NS). In SCN5A+ patients, HNE-modified protein-positive area was not significantly different between the VF+ and VF− group (VF+ group: 14.0±8.8% vs. VF− group: 12.7±7.5%, P=NS) (Fig. 3B). However, in patients without SCN5A (SCN5A−), the area was significantly larger in the VF+ group than that in the VF−

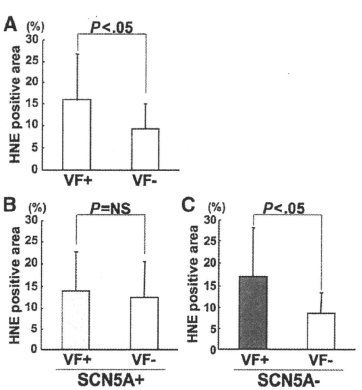

Fig. 3. HNE-modified protein-positive area. (A) HNE-modified protein-positive area in patients with spontaneous VF (VF+ group) vs. without (VF− group). (B) HNE-modified protein-positive area in patients with SCN5A mutation (SCN5A+). (C) HNE-modified protein-positive area in patients without SCN5A mutation (SCN5A−). Data are expressed as means±S.D.

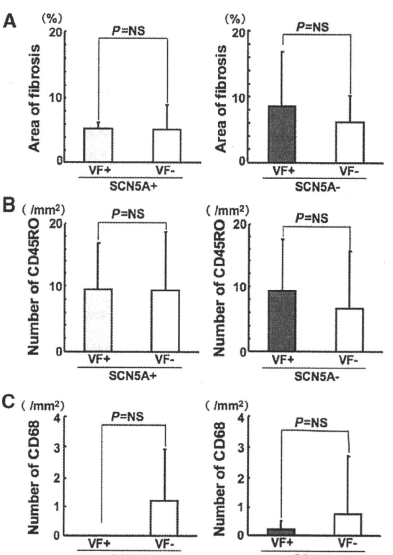

Fig. 4. Histological and immunohistochemical analyses. (A) Areas of fibrosis in SCN5A+ and SCN5A− patients in the VF+ and VF− groups. (B) Numbers of CD45RO-positive cells in SCN5A+ and SCN5A− patients in the VF+ and VF− groups. (C) Numbers of CD68-positive cells. Data are expressed as means±S.D.

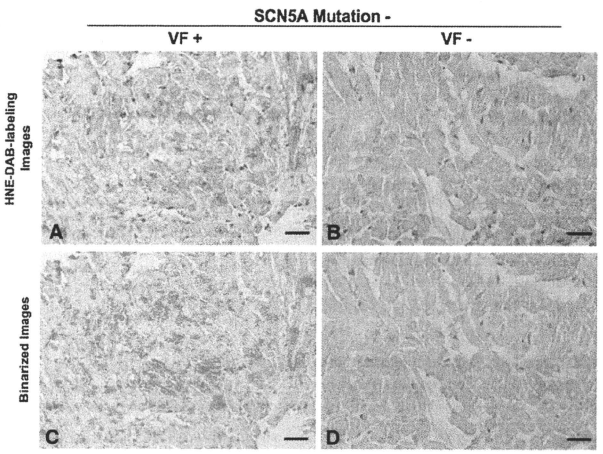

Fig. 5. Representative figures of HNE-modified protein staining. Representative immunostainings (brown) for HNE-modified protein by diaminobenzidine (DAB) (A and B) and binarized images (green) using WinROOF Image software (C and D) in the myocardium from a patient without SCN5A mutation and with spontaneous VF (A and C) and from a patient without SCN5A mutation and without spontaneous VF (B and D).

group (VF+ group: 17.0±11.2% vs. VF− group: 8.4±4.9%, $P<.05$) (Fig. 3C).

Area of fibrosis was not different between the VF+ and VF− groups in both SCN5A+ and SCN5A− patients (Fig. 4A). The number of CD45RO-positive cells was not significantly different between the VF+ and VF− groups in both SCN5A+ and SCN5A− patients (Fig. 4B). Infiltration of CD68-positive cell was rarely seen in patients in both the VF+ and VF− groups with or without SCN5A mutation (Fig. 4C).

Fig. 5 shows representative immunostainings (A and B) for HNE-modified protein in the myocardium from a patient without SCN5A mutation and with spontaneous VF (A and C) and from a patient without SCN5A mutation and without spontaneous VF (B and D). Positive immunostainings (brown) for HNE-modified protein are distinct in the cytosol of cardiac myocytes from a patient with spontaneous VF (Fig. 5A).

4. Discussion

We investigated oxidative stress levels in the myocardia of patients with Brugada-type ECG and also examined the relationship between oxidative stress levels and VF episodes. The major new finding of this work is that oxidative stress is elevated in the myocardium of patients with Brugada-type ECG who have VF episodes and do not have SCN5A gene mutations. Oxidative stress may play an important role in the occurrence of VF in patients with Brugada-type ECG without SCN5A gene mutations.

Oxidative stress induces loss of function of I_{Na}. Shang et al. [10] reported that H_2O_2 decreases SCN5A mRNA transcription and I_{Na} current. Fukuda et al. [11] reported that E2-isoketal, a highly reactive product of lipid peroxidation, potentiates inactivation of cardiac Na^+ channels. Our data showed that oxidative stress was elevated in the myocardium of BS patients with VF episodes who do not have SCN5A gene mutations. These findings indicated that loss of function of I_{Na} caused by oxidative stress is associated with the occurrence of VF in patients with Brugada-type ECG.

Oxidative stress is not related to the occurrence of VF in patients with Brugada-type ECG who have SCN5A mutation in our study. Frustaci et al. [9] reported that carriers of SCN5A mutations demonstrate myocardial cell degeneration and death. Therefore, mechanisms of VF occurrence in Brugada-type ECG patients with SCN5A mutation may be different from those in patients without SCN5A mutation. Further studies are needed to clarify the mechanisms. Since HNE-modified protein-positive areas were not significantly different in the SCN5A+ and SCN5A− patients in our study, it was thought that loss of function of the sodium channel due to SCN5A mutation did not cause oxidative stress.

ROS cause damage to lipid cell membranes in the process of lipid peroxidation. In this process, several aldehydes, including HNE, are generated as final products. HNE is recognized as the most reliable marker of lipid peroxidation [13,14]. Furthermore, exposure to a large amount of HNE (400 μmol/l) increases rat cardiac Na^+ current and causes cytotoxic effects in cardiac myocytes [21,22]. However, a small amount of HNE does not have any detectable gating

effects on I_{Na}, including I_{Na} decay, voltage-dependent activation, or the voltage dependence of channel availability [11]. Cardiac function is normal in patients with BS. Therefore, HNE in cardiac myocytes in patients with BS is thought to be at a low level and to have no cytotoxic effects and/or effect on I_{Na} current.

In conclusion, oxidative stress is elevated in the myocardium of patients with Brugada-type ECG who have VF episodes and do not have SCN5A gene mutations compared to that in the myocardium of patients without VF episodes. Loss of function of I_{Na} caused by oxidative stress may be a mechanism for VF in patients with Brugada-type ECG who do not have SCN5A mutation. Further studies are needed to clarify this point.

Acknowledgments

We thank Kaoru Kobayashi, Miyuki Fujiwara, and Masayo Ohmori (Okayama University) for their excellent secretarial assistance.

References

[1] Brugada P, Brugada J. Right bundle branch block, persistent ST segment elevation and sudden cardiac death: a distinct clinical and electrocardiographic syndrome. A multicenter report. J Am Coll Cardiol 1992;20:1391–6.

[2] Chen Q, Kirsch GE, Zhang D, Brugada R, Brugada J, Brugada P, et al. Genetic basis and molecular mechanism for idiopathic ventricular fibrillation. Nature 1998;392:293–6.

[3] Miura D, Nakamura K, Ohe T. Update on genetic analysis in Brugada syndrome. Heart Rhythm 2008;5:1495–6.

[4] Antzelevitch C, Pollevick GD, Cordeiro JM, Casis O, Sanguinetti MC, Aizawa Y, et al. Loss-of-function mutations in the cardiac calcium channel underlie a new clinical entity characterized by ST-segment elevation, short QT intervals, and sudden cardiac death. Circulation 2007;115:442–9.

[5] London B, Michalec M, Mehdi H, Zhu X, Kerchner L, Sanyal S, et al. Mutation in glycerol-3-phosphate dehydrogenase 1 like gene (GPD1-L) decreases cardiac Na+ current and causes inherited arrhythmias. Circulation 2007;116:2260–8.

[6] Watanabe H, Koopmann TT, Le Scouarnec S, Yang T, Ingram CR, Schott JJ, et al. Sodium channel beta1 subunit mutations associated with Brugada syndrome and cardiac conduction disease in humans. J Clin Invest 2008.

[7] Delpón E, Jonathan MC, Núñez L, Thomsen PEB, Guerchicoff A, Pollevick GD, et al. Functional effects of KCNE3 mutation and its role in the development of Brugada syndrome. Circ Arrhythmia Electrophysiol 2008;1:209–18.

[8] Makiyama T, Akao M, Haruna Y, Tsuji K, Doi T, Ohno S, et al. Mutation analysis of the glycerol-3 phosphate dehydrogenase-1 like (GPD1L) gene in Japanese patients with Brugada syndrome. Circ J 2008.

[9] Frustaci A, Priori SG, Pieroni M, Chimenti C, Napolitano C, Rivolta I, et al. Cardiac histological substrate in patients with clinical phenotype of Brugada syndrome. Circulation 2005;112:3680–7.

[10] Shang LL, Sanyal S, Pfahnl AE, Jiao Z, Allen J, Liu H, et al. NF-kappaB-dependent transcriptional regulation of the cardiac scn5a sodium channel by angiotensin II. Am J Physiol Cell Physiol 2008; 294:C372–9.

[11] Fukuda K, Davies SS, Nakajima T, Ong BH, Kupershmidt S, Fessel J, et al. Oxidative mediated lipid peroxidation recapitulates proarrhythmic effects on cardiac sodium channels. Circ Res 2005;97: 1262–9.

[12] Danson EJ, Paterson DJ. Reactive oxygen species and autonomic regulation of cardiac excitability. J Cardiovasc Electrophysiol 2006;17 (Suppl 1):S104–12.

[13] Nakamura K, Kusano K, Nakamura Y, Kakishita M, Ohta K, Nagase S, et al. Carvedilol decreases elevated oxidative stress in human failing myocardium. Circulation 2002;105:2867–71.

[14] Nakamura K, Kusano KF, Matsubara H, Nakamura Y, Miura A, Nishii N, et al. Relationship between oxidative stress and systolic dysfunction in patients with hypertrophic cardiomyopathy. J Card Fail 2005;11: 117–23.

[15] Morita H, Morita ST, Nagase S, Banba K, Nishii N, Tani Y, et al. Ventricular arrhythmia induced by sodium channel blocker in patients with Brugada syndrome. J Am Coll Cardiol 2003;42:1624–31.

[16] Morita H, Kusano KF, Miura D, Nagase S, Nakamura K, Morita ST, et al. Fragmented QRS as a marker of conduction abnormality and a predictor of prognosis of Brugada syndrome. Circulation 2008;118: 1697–704.

[17] Kobayashi M, Nakamura K, Kusano KF, Nakamura Y, Ohta-Ogo K, Nagase S, et al. Expression of monocyte chemoattractant protein-1 in idiopathic dilated cardiomyopathy. Int J Cardiol 2008;126:427–9.

[18] Wang Q, Shen J, Li Z, Timothy K, Vincent GM, Priori SG, et al. Cardiac sodium channel mutations in patients with long QT syndrome, an inherited cardiac arrhythmia. Hum Mol Genet 1995; 4:1603–7.

[19] Tada T, Kusano KF, Nagase S, Banba K, Miura D, Nishii N, et al. Clinical significance of macroscopic T-wave alternans after sodium channel blocker administration in patients with Brugada syndrome. J Cardiovasc Electrophysiol 2008;19:56–61.

[20] Kusano KF, Taniyama M, Nakamura K, Miura D, Banba K, Nagase S, et al. Atrial fibrillation in patients with Brugada syndrome relationships of gene mutation, electrophysiology, and clinical backgrounds. J Am Coll Cardiol 2008;51:1169–75.

[21] Bhatnagar A. Electrophysiological effects of 4-hydroxynonenal, an aldehydic product of lipid peroxidation, on isolated rat ventricular myocytes. Circ Res 1995;76:293–304.

[22] Nakamura K, Miura D, Kusano KF, Fujimoto Y, Sumita-Yoshikawa W, Fuke S, et al. 4-Hydroxy-2-nonenal induces calcium overload via the generation of reactive oxygen species in isolated rat cardiac myocytes. J Card Fail 2009;15:709–16.

Hypertension
JOURNAL OF THE AMERICAN HEART ASSOCIATION

American Heart Association®
Learn and Live℠

Left Atrial Volume Combined With Atrial Pump Function Identifies Hypertensive Patients With a History of Paroxysmal Atrial Fibrillation

Norihisa Toh, Hideaki Kanzaki, Satoshi Nakatani, Takahiro Ohara, Jiyoong Kim, Kengo F. Kusano, Kazuhiko Hashimura, Tohru Ohe, Hiroshi Ito and Masafumi Kitakaze

Hypertension 2010;55;1150-1156; originally published online Apr 5, 2010;
DOI: 10.1161/HYPERTENSIONAHA.109.137760
Hypertension is published by the American Heart Association. 7272 Greenville Avenue, Dallas, TX 72514
Copyright © 2010 American Heart Association. All rights reserved. Print ISSN: 0194-911X. Online ISSN: 1524-4563

The online version of this article, along with updated information and services, is located on the World Wide Web at:
http://hyper.ahajournals.org/cgi/content/full/55/5/1150

Subscriptions: Information about subscribing to Hypertension is online at
http://hyper.ahajournals.org/subscriptions/

Permissions: Permissions & Rights Desk, Lippincott Williams & Wilkins, a division of Wolters Kluwer Health, 351 West Camden Street, Baltimore, MD 21202-2436. Phone: 410-528-4050. Fax: 410-528-8550. E-mail:
journalpermissions@lww.com

Reprints: Information about reprints can be found online at
http://www.lww.com/reprints

Downloaded from hyper.ahajournals.org at OKAYAMA UNIV on May 2, 2011

Left Atrial Volume Combined With Atrial Pump Function Identifies Hypertensive Patients With a History of Paroxysmal Atrial Fibrillation

Norihisa Toh, Hideaki Kanzaki, Satoshi Nakatani, Takahiro Ohara, Jiyoong Kim, Kengo F. Kusano, Kazuhiko Hashimura, Tohru Ohe, Hiroshi Ito, Masafumi Kitakaze

Abstract—Identifying patients at high risk for the occurrence of atrial fibrillation is one means by which subsequent thromboembolic complications may be prevented. Left atrial enlargement is associated with progression of atrial remodeling, which is a substrate for atrial fibrillation, but impaired atrial pump function is also another aspect of the remodeling. Our objective was to differentiate patients with a history of paroxysmal atrial fibrillation using echocardiography. We studied 280 hypertensive patients (age: 66±7 years; left ventricular ejection fraction: 65±8%), including 140 consecutive patients with paroxysmal atrial fibrillation and 140 age- and sex-matched control subjects. Left atrial volume was measured using the modified Simpson method at both left ventricular end systole and preatrial contraction and was indexed to body surface area. Peak late-diastolic mitral annular velocity was measured during atrial contraction using pulsed tissue Doppler imaging as an atrial pump function. Left atrial volume index measured at left ventricular end systole had a 74% diagnostic accuracy and a 71% positive predictive value for identifying patients with paroxysmal atrial fibrillation; these values for the ratio of left atrial volume index at left ventricular end systole to the peak late-diastolic mitral annular velocity were 82% and 81%, respectively, and those for the ratio of left atrial volume index at preatrial contraction to the peak late-diastolic mitral annular velocity were 86% and 90%, respectively. In conclusion, left atrial size combined with atrial pump function enabled a more accurate diagnosis of a history of paroxysmal atrial fibrillation than conventional parameters. (***Hypertension.*** **2010;55:1150-1156.)**

Key Words: hypertension ■ echocardiography ■ atrial fibrillation ■ left atrium ■ remodeling

Atrial fibrillation (AF) is not generally life threatening but is considered to be the most common cause of ischemic stroke, which often yields serious complications because of acute occlusion of intracranial arteries without collateral circulation. The incidence of stroke is increased by ≈5-fold in the presence of nonvalvular AF.[1–5] Moreover, recent studies have demonstrated that stroke risk is no less in patients with paroxysmal AF (PAF) than in those with persistent AF.[6] Therefore, it is crucial to identify patients who have PAF in order to prevent subsequent thromboembolic complications, especially in patients with hypertension, which is a major etiologic factor associated with both AF and stroke.[7–9]

Left atrial (LA) enlargement associated with the progression of atrial structural remodeling plays a key role in the initiation and maintenance of AF.[10,11] The most recent recommendations for echocardiographic chamber quantification indicate that LA volume (LAV) provides an accurate measurement of asymmetrical remodeling of the LA chamber.[12] LAV is increased in patients with PAF[13] and is also an important predictor of cardiovascular outcome, including the occurrence of AF,[14] supporting the concept that LAV is a hallmark of atrial remodeling.

In patients with PAF, Doppler transmitral flow velocity and tissue Doppler imaging (TDI)–derived mitral annulus velocity during atrial contraction, which are considered to reflect atrial pump function,[15–20] have been reported to be decreased compared with those in control subjects.[13,16,21] According to the Frank-Starling law, atrial pump function is also enhanced with an increase in LAV; however, excessive LA enlargement leads to atrial dysfunction.[22,23] Accordingly, we hypothesized that adding information on atrial pump function may provide a better marker of atrial remodeling.

In the present study, we aimed to differentiate patients with a history of PAF among those with hypertension more accurately by means of LAV combined with atrial pump function.

Methods

Study Population

Patients referred to our laboratory were classified into the PAF group if they met the following criteria: (1) ≥1 episode of self-terminating

Received June 18, 2009; first decision July 6, 2009; revision accepted March 8, 2010.

From the Cardiovascular Division of Medicine (N.T., H.K., S.N., T.O., J.K., K.H., M.K.), National Cardiovascular Center, Osaka, Japan; Department of Cardiovascular Medicine (K.F.K., H.I.), Okayama University Graduate School of Medicine, Dentistry, and Pharmaceutical Sciences, Okayama, Japan; Department of Cardiology (T.O.), Sakakibara Heart Institute of Okayama, Okayama, Japan.

Correspondence to Hideaki Kanzaki, Cardiovascular Division of Medicine, National Cardiovascular Center, 5-7-1 Fujishiro-dai, Suita, Osaka 565-8565, Japan. E-mail kanzakih@hsp.ncvc.go.jp

© 2010 American Heart Association, Inc.

Hypertension **is available at http://hyper.ahajournals.org** **DOI: 10.1161/HYPERTENSIONAHA.109.137760**

Downloaded from hyper.ahajournals.org by OKAYAMA UNIV on May 2, 2011

PAF documented by a 12-lead ECG, 24-hour Holter monitoring, or continuous monitoring during hospitalization without taking any antiarrhythmic drugs and having been free from arrhythmic episodes for >1 week before undergoing echocardiography; (2) hypertension (systolic blood pressure ≥140 mm Hg and/or diastolic blood pressure ≥90 mm Hg or treatment for hypertension); (3) less than moderate mitral regurgitation; (4) sinus rhythm during echocardiography; (5) no medical history of other arrhythmias (including persistent AF), valvular heart disease (including mitral annular calcification), heart failure, ischemic heart disease, cardiomyopathy, cardiac surgery, thyroid disease, or pulmonary disease; and (6) age between 40 and 80 years.

Control subjects were recruited from a clinical health examination in Arita, Japan. All of the attendees underwent a formal medical history interview, ECG, and physical and laboratory examinations. Blood pressure was measured at each of ≥2 visits to the office, and the average of ≥2 seated blood pressures was used according to established recommendations.[24] Of the attendees who also underwent echocardiography, age- and sex-matched subjects who met criteria 2 through 6 were classified as the control group. The study was approved by the institutional review board, and the study was conducted in accordance with the ethical principles of the Declaration of Helsinki. All of the subjects provided informed consent.

Echocardiography

All of the echocardiographic studies were performed with either a Vivid 7 Dimension (GE Healthcare) or Aplio XV (Toshiba Medical Systems) ultrasound system. Cardiac chamber size, left ventricular (LV) ejection fraction (LVEF), LV mass, and LA dimension were evaluated according to the recommendations of the American Society of Echocardiography.[12] LAV was measured using the biplane modified Simpson's method at the ventricular end-systolic frame just before the mitral valve opening from apical 4- and 2-chamber views. Strictly speaking, however, LA does not contract from the size of LAV at ventricular end systole. Thus, preatrial contraction LAV (LAV_{preA}) was also obtained from the last frame just before mitral valve reopening. Active LA emptying fraction (active LAEF) was calculated by the following formula: $(LAV_{preA}-LAV_{min})/LAV_{preA}\times100\%$, where LAV_{min} is the minimal LAV at atrial end systole. All of the LAVs were indexed to body surface area as LAVi, $LAVi_{preA}$, and $LAVi_{min}$, respectively. LV mass was also indexed to body surface area (LV mass index). LV hypertrophy was defined as LV mass index >104 g/m^2 in women and >116 g/m^2 in men.[25]

The sample volume of pulsed-wave Doppler imaging was placed at the tip level of the mitral leaflets in the apical 4-chamber view. Then the peak mitral inflow early diastolic and atrial filling (E and A) velocities and the E-wave deceleration time were obtained. The sample volume of the pulsed TDI was placed at the septal and lateral margins of the mitral annulus. Peak early and late-diastolic mitral annular velocities were measured, and then the average values of septal and lateral velocities were used as Ea and Aa, respectively. E/Ea was calculated as a surrogate for the LV filling pressure.[26]

Statistical Analysis

Data are expressed as mean±SD. An ANOVA was performed to test for statistically significant differences between 2 unpaired mean values, and categorical data and percentage frequencies were analyzed by the χ^2 test. Correlations were determined with Pearson product moment correlation analysis. Receiver operating characteristic (ROC) curves were constructed to determine the optimal sensitivity and specificity. The area under the curve (AUC) was calculated to assess the overall performance of various variables for the detection of PAF. Univariate and multivariate logistic regression analyses were performed to characterize diagnostic factors of a history of PAF. Variables considered included age, sex, body weight, LV hypertrophy, E/Ea, and diabetes mellitus. A scatter diagram was used to illustrate the relationship between LA size and LA pump function in each patient. A straight line was drawn passing through the origin to discriminate the best between the PAF and control groups, and another line was drawn to establish the boundary above which spots belonging to the PAF group existed. The slope indicates the ratio of LA size to LA pump function: the former corresponds to the optimal cutoff value from the ROC analysis and the latter is the minimum of the ratios of the PAF group. Most statistical tests were performed with SPSS version 12.0 (SPSS Inc). The calculation and comparison of AUC values and the logistic regression analyses were performed with Stata SE version 8.2 (Stata Corp). A P value <0.05 was considered to be statistically significant. The statistical power of the present study was finally calculated.

Forty subjects were randomly selected from each group and analyzed blindly by 2 authors (N.T. and H.K.) to assess reproducibility. The interobserver and intraobserver variabilities were, respectively, 4.0% and 3.8% for LAV, 4.2% and 4.2% for LAV_{preA}, 12.3% and 9.9% for LAV_{min}, 4.4% and 4.1% for peak A velocity, 3.6% and 3.5% for septal Aa, and 4.0% and 3.7% for lateral Aa.

Table 1. Clinical Characteristics of the Study Population

Variable	Control Group (n=140)	PAF Group (n=140)
Age, y	66±7	66±8
Women, %	47	47
Height, cm	158±9	160±10
Weight, kg	58±10	60±10
Body surface area, m^2	1.59±0.17	1.60±0.26
Body mass index, kg/m^2	23.2±3.3	23.6±3.0
Systolic blood pressure, mm Hg	140±18	137±16
Diastolic blood pressure, mm Hg	82±10	80±11
Diabetes mellitus, %	17	21
Hyperlipidemia, %	46	47
Smoking, %	31	23
Concomitant cardiovascular therapies		
ACE inhibitors, %	7	5
ARBs, %	30	32
β-Blockers, %	18	27
Calcium channel blockers, %	32	37

Values are expressed as mean±SD unless otherwise specified. ACE indicates angiotensin-converting enzyme; ARB, angiotensin II receptor blockers. No significant differences were found between groups.

Results

Clinical and Echocardiographic Characteristics

A total of 280 subjects with hypertension (mean age: 66±7 years; range: 40 to 80 years; 148 men; LVEF: 65±8%) were enrolled in the present study. There were no significant differences in clinical parameters or the use of antihypertensive drugs between the 140 control and 140 PAF subjects (Table 1). The median time interval between the first PAF episode and this examination was 2.0 years (25th to 75th percentile: 0.2 to 7.0 years), and 62% of the patients with PAF were symptomatic. Echocardiographic characteristics are depicted in Table 2. No significant group differences were found for the following parameters: LV end-diastolic diameter, LV end-systolic diameter, and LVEF. LV mass index, LA dimension, and indices related to the LAV were significantly increased in the PAF group compared with those in the control group, whereas active LAEF was decreased in the PAF group. The prevalences of LV hypertrophy were 45% in the PAF group (37 women and 25 men) and 28% in the control group (18 women and 21 men). The E-wave decel-

Downloaded from hyper.ahajournals.org at OKAYAMA UNIV on May 2, 2011

Table 2. Echocardiographic Characteristics of the Study Population

Variable	Control Group (n=140)	PAF Group (n=140)	*P*
LV end-diastolic dimension, mm	47±5	46±5	0.114
LV end-systolic dimension, mm	28±5	28±5	0.445
LVEF, %	65±8	65±8	0.839
LV mass index, g/m^2	100±20	112±27	<0.001
LA dimension, mm	38±5	43±5	<0.001
LAVi, ml/m^2	30±7	42±12	<0.001
$LAVi_{preA}$, ml/m^2	21±6	32±10	<0.001
$LAVi_{min}$, ml/m^2	14±4	25±10	<0.001
Active LAEF, %	34±8	23±10	<0.001
Peak E velocity, cm/s	64±15	70±19	0.007
Peak A velocity, cm/s	80±18	67±21	<0.001
E/A	0.85±0.24	1.18±0.67	<0.001
E-wave deceleration time, ms	233±44	224±49	0.069
Ea, cm/s	7.5±1.9	6.8±1.9	<0.001
Aa, cm/s	11.1±2.3	7.7±2.6	<0.001
E/Ea	9.0±2.5	11.1±4.3	<0.001
LAVi/A, mL · m^{-2}/cm · s^{-1}	0.39±0.11	0.72±0.41	<0.001
LAVi/Aa, mL · m^{-2}/cm · s^{-1}	2.9±1.0	6.8±5.1	<0.001
$LAVi_{preA}$/active LAEF	0.64±0.28	1.96±2.23	<0.001
$LAVi_{preA}$/A, mL · m^{-2}/cm · s^{-1}	0.27±0.08	0.55±0.36	<0.001
$LAVi_{preA}$/Aa, mL · m^{-2}/cm · s^{-1}	1.9±0.4	5.3±4.3	<0.001

Values are expressed as mean±SD.

eration time was comparable, but peak E velocity was significantly greater, and peak A velocity was less in the PAF group than in the control group. The Ea and Aa were lower in the PAF group than in the control group. E/Ea was greater in the PAF group than in the control group.

The following correlations were found: (1) LAVi and $LAVi_{preA}$ were correlated with E/Ea (LAVi: r=0.418, P<0.001; $LAVi_{preA}$: r=0.416, P<0.001); (2) LAVi and $LAVi_{preA}$ were correlated with LV mass index (LAVi: r=0.440, P<0.001; $LAVi_{preA}$: r=0.459, P<0.001); (3) LAVi was strongly correlated with the $LAVi_{preA}$ (r=0.916; P<0.001); (4) Aa was correlated well with active LAEF (r=0.755; P<0.001) and this correlation was still observed in patients with severely enlarged LA (r=0.775; P<0.001), which is defined as LAVi >40 mL/m^2 in the recommendations[12]; and (5) LAVi/Aa and $LAVi_{preA}$/Aa were correlated with the time interval between the first PAF episode and this examination (LAVi/Aa: r=0.267, P=0.012; $LAVi_{preA}$/Aa: r=0.275, P=0.009).

Echocardiographic Detection of PAF Among Hypertensive Patients

Various parameters, listed in Table 3, were examined using ROC analysis. $LAVi_{preA}$/Aa was best for detecting patients with a history of PAF considering the AUC. The AUC of $LAVi_{preA}$/Aa was statistically greater than those of the $LAVi_{preA}$/A, $LAVi_{preA}$/active LAEF, LAVi/Aa, and LAVi values (P=0.024, P=0.003, P<0.001, and P<0.001, respectively). Although the statistical power calculated was 76% because of the limited number of subjects, statistically significant differences were found between the $LAVi_{preA}$/Aa ratio and other parameters. The ROC curves for the $LAVi_{preA}$/Aa, LAVi/Aa, LAVi, and LA dimension are shown in Figure 1.

Table 3. AUCs for Echocardiographic Variables

Variable	AUC	SE	95% CI
LA dimension	0.733	0.030	0.675 to 0.791
LAVi	0.820	0.024	0.772 to 0.868
$LAVi_{preA}$	0.861	0.022	0.819 to 0.904
LAVi/A	0.852	0.023	0.807 to 0.898
LAVi/Aa	0.884	0.019	0.847 to 0.922
$LAVi_{preA}$/active LAEF	0.893	0.019	0.856 to 0.930
$LAVi_{preA}$/A	0.888	0.020	0.849 to 0.927
$LAVi_{preA}$/Aa	0.927	0.015	0.897 to 0.956

The sensitivity, specificity, diagnostic accuracy, and positive predictive value for the detection of PAF were determined with an optimal cutoff value according to the ROC analysis, as shown in Table 4. Diagnostic accuracy and positive predictive value of the $LAVi_{preA}$/Aa ratio at the cutoff value of >2.7 mL · m^{-2}/cm · s^{-1} were clearly superior to those of the LAVi of >32.0 mL/m^2.

From the results of univariate analysis for age, sex, body weight, LV hypertrophy, E/Ea, and diabetes mellitus, LV hypertrophy (odds ratio: 2.059 [95% CI: 1.251 to 3.386]; P<0.001) and E/Ea (odds ratio: 1.205 [95% CI: 1.108 to 1.309]; P<0.001) were considered as significant covariates. However, multivariate analysis demonstrated that the $LAVi_{preA}$/Aa ratio was the single significant factor of a history of PAF (odds ratio: 11.786 [95% CI: 6.178 to 22.483]; P<0.001).

LA Size Against Atrial Pump Function

The relationship between LA size and atrial pump function in our population is illustrated in Figure 2. LA size and Aa showed an inverse correlation (LAVi: r=−0.503, P<0.001; $LAVi_{preA}$:

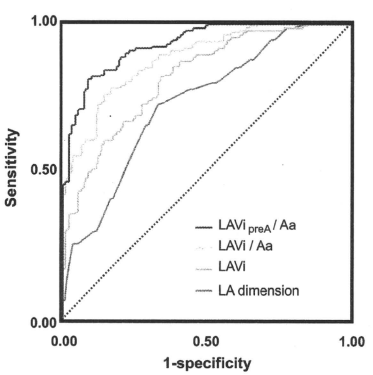

Figure 1. ROC curves for detecting PAF. Comparison of ROC curves for the $LAVi_{preA}$/Aa (red line), LAVi/Aa (yellow line), LAVi (green line), and LA dimension (blue line) values. The AUC values are listed in Table 3.

Downloaded from hyper.ahajournals.org at OKAYAMA UNIV on May 2, 2011

Table 4. Evaluation of Echocardiographic Parameters According to Sensitivity, Specificity, and Diagnostic Accuracy for Detection of PAF in Hypertensive Patients

Variable	Sensitivity, %	Specificity, %	Diagnostic Accuracy, %	PPV, %
LA dimension >41 mm	72	67	71	69
LAVi >32.0 mL/m^2	82	66	74	71
LAVi/A >0.50 mL · m^{-2}/cm · s^{-1}	75	87	81	85
LAVi/Aa >3.6 mL · m^{-2}/cm · s^{-1}	78	84	82	81
$LAVi_{preA}$/A >0.36 mL · m^{-2}/cm · s^{-1}	80	85	83	84
$LAVi_{preA}$/Aa >2.7 mL · m^{-2}/cm · s^{-1}	82	91	86	90

Values are expressed as percentage. PPV indicates positive predictive value.

$r=-0.458$, $P<0.001$). The PAF group is located disproportionately in the upper left part as compared with the control group. The black dotted lines discriminate best between the PAF and control groups, with slopes of 3.6 (the LAVi/Aa ratio=3.6 mL · m^{-2}/cm · s^{-1}) and 2.7 (the $LAVi_{preA}$/Aa ratio=2.7 mL · m^{-2}/cm · s^{-1}), respectively. The red dotted lines show the lower bound of the PAF group, with slopes of 2.3 and 1.9, respectively.

Discussion

The LA of hypertensive patients with PAF was characterized by further enlargement and impaired pump function as compared with that of hypertensive patients in whom PAF had never been documented. Thus, the ratio of $LAVi_{preA}$ to Aa was most powerful, and the ratio of LAVi to Aa was the next most powerful for differentiating hypertensive patients with a history of PAF.

LA Remodeling in Hypertension

LA size has been reported to serve as a surrogate measure of chronic LV diastolic dysfunction.[27] Hypertension induces an increase in LV wall stress, leading to increased wall thickness, myocyte hypertrophy, and myocardial fibrosis.[28,29] Impaired myocardial relaxation and increased LV diastolic stiffness can cause elevated LV diastolic filling pressure,[30] consistent with the increase in E/Ea. Moreover, long-standing hypertension results in interstitial fibrosis and arrhythmic substrate even in the LA.[31] In a large cohort study, increased LV mass and LA diameter were independently associated with the occurrence of AF in patients with hypertension.[32] Similarly, we found that LV mass index, E/Ea, and LAVi values were significantly increased in our hypertensive patients with PAF compared with those in hypertensive patients without PAF. In addition, LAVi showed a significant correlation with both LV mass index and E/Ea. These findings do not contradict the concept that the occurrence of PAF in hypertension is associated with LA remodeling as a consequence of LA overload because of elevated LV filling pressure.

The $LAVi_{preA}$/Aa and LAVi/Aa ratios showed a very modest but yet significant correlation with the time interval between the first PAF episode and this examination. LA remodeling is thought to progress according to not only the LA overload but also the duration of AF.[33] Thus, the indices that we proposed may be markers representing the degrees of progressive LA remodeling.

Frank-Starling Mechanism of LA Function

According to the Frank-Starling mechanism, contractile force of the ventricular myocardium is proportional to its initial length; this mechanism also applies to the LA myocardium.[22,23] LA pump function is enhanced in response to elevated LV filling pressure as long as the Frank-Starling mechanism holds. Within the range of compensation, therefore, the points in Figure 2 should range toward the upper right direction; in contrast, the points belonging to the PAF group are located in the upper left area. This disproportional distribution is also thought to demonstrate a shift of or a deviation from the Frank-Starling curves because of further progression of atrial remodeling in the PAF group. In addition, Figure 2 shows that patients with an LAVi/Aa ratio ≥2.3 mL · m^{-2}/cm · s^{-1}

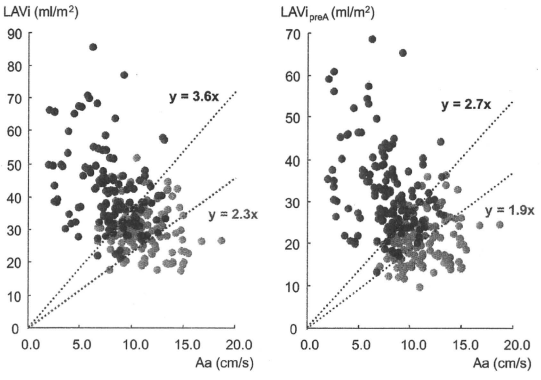

Figure 2. Relationship between LA size and pump function in patients with and without PAF. Scatter diagrams showing the distribution of plots of the LAVi against Aa values (left) and $LAVi_{preA}$ against Aa values (right). Red points indicate hypertensive patients with PAF, and blue points indicate hypertensive patients in whom PAF has never been documented. Patients with LAVi/Aa ratios >2.3 mL · m^{-2}/cm · s^{-1} or $LAVi_{preA}$/Aa ratios >1.9 mL · m^{-2}/cm · s^{-1} may have PAF.

Downloaded from hyper.ahajournals.org at OKAYAMA UNIV on May 2, 2011

or $LAVi_{preA}/Aa$ ratio ≥ 1.9 mL · m^{-2}/cm · s^{-1} may potentially have a history of PAF.

Preload is originally reflected as the initial stretching of cardiac myocytes before contraction. Thus, when adding atrial function to LA size for assessing atrial remodeling, $LAVi_{preA}$ is thought to be physiologically more preferable to LA size than is LAVi. Therefore, it was a reasonable result that the $LAVi_{preA}/Aa$ ratio showed better diagnostic ability than the LAVi/Aa ratio.

Measurement of Atrial Pump Function

Several past studies have demonstrated that Aa velocity correlates well with atrial contractile function and can be used as a rapid and accurate marker of atrial function.[16–20] Similar to results of these studies, Aa showed a significant correlation with active LAEF in our study, and the correlation of Aa with active LAEF also remained in patients with excessive LA enlargement.

The changes in flow velocity profile with different positions of the pulsed-wave Doppler sample volume may affect the diagnostic accuracy of the $LAVi_{preA}/A$ ratio. Even slight changes in sample volume position can easily cause a decrease in peak A velocity.[34] In contrast, TDI-derived mitral annulus velocities are relatively independent of these problems.[35] Our results also show that Aa is a marker reflecting atrial pump function.

Lateral Aa is a favorable discrimination parameter because its amplitude is greater than that of septal Aa. However, the left lung often attenuates tissue Doppler signals from the lateral annulus margin. The mitral septal annulus motion is always parallel to the Doppler beam, and its measurements are certain. Septal Aa could, however, be influenced by right atrial pump function. In the present study, therefore, we used the average of the septal and lateral Aas.

Study Limitations

First, this was a cross-sectional study. To clarify whether the present index can predict future AF development or complications, further research must provide longitudinal assessments. Second, it is difficult to distinguish whether the impaired atrial pump function was attributed to LA remodeling or showed a recovery process after spontaneous conversion of AF. This issue does not concern the diagnosis of PAF, but it may slightly affect the cutoff value for detecting PAF. Third, atrial reservoir function was not examined in the present study. Some reports indicate that evaluating LA reservoir function using strain or strain rate is useful for the prediction of AF relapse after treatments.[36,37] Nevertheless, we chose to use pulsed TDI parameters for the following reasons: (1) measurement of strain or strain rate with high reproducibility or using the speckle tracking method requires a high-end ultrasound machine and special dedicated software, but pulsed TDI is available on almost all machines; (2) peak late-diastolic atrial strain rate during atrial contraction has been reported to be correlated well with Aa[38,39]; (3) speckle tracking software, which is used when measuring atrial strain or strain rate, is designed primarily for the LV and not the LA; and (4) atrial strain or strain rate reflects only regional function of the LA, and the position of regions of interest for assessing LA global pump function is still controversial, whereas Aa is a marker of atrial global function and has been validated by cardiac catheters.[17] We preferred this general technology because our goal was to make our method accessible. Fourth, we did not measure pulmonary venous flow for assessing LV diastolic function because obtaining an adequate signal for analysis has been reported to be difficult in all subjects.[40,41] Furthermore, a recent consensus statement recommends tissue Doppler velocities as a first-line echocardiographic diagnostic approach to LV diastolic dysfunction.[42] Fifth, obtaining an accurate time interval between the first PAF episode and the current examination was practically difficult because PAF is, by nature, an elusive disease, and the majority of PAF episodes are known to be asymptomatic.[43] Similarly, the first PAF episode in asymptomatic patients was noticed incidentally as an irregularly irregular rhythm during auscultation or palpitating arterial pulse and was confirmed using ECG at a monthly or biweekly consultation day; thus, the interval may be not accurate. Little information on the number and duration of PAF episodes was available in the present study. Finally, we cannot clearly state that self-terminating spontaneous AF was never present in hypertensive patients with PAF within 1 week of examination or in patients with hypertension alone; nonetheless, we addressed this concern by performing repeated 12-lead ECGs, 24-hour Holter monitoring, and strict medical interviews for the subjects of the study.

Perspectives

Our observations that the LA of hypertensive patients with PAF is characterized by dilatation and impaired pump function and that the ratio of LA size to pump function is useful for identifying patients with PAF have important public health and clinical implications. If the presence of PAF is suspected at the time of echocardiography, further examinations and careful monitoring (including repeated 24-hour or event-ECG Holter recording) may be considered. This is especially true for patients with multiple risk factors for stroke (eg, congestive heart failure, hypertension, age >75 years, diabetes mellitus, and previous stroke or transient ischemic attack). In other words, the present indices may be useful for recommending preventive therapy in high-risk patients, because clinicians can prevent the greater part of ischemic stroke from AF with anticoagulation therapy.[44] A recent report from the Framingham Heart Study proposed a risk score for the future development of AF, but echocardiographic parameters provided only slight improvement in the risk assessment score.[45] The measurements derived from the conventional M-mode method may have attenuated the benefits of echocardiography in the aforementioned study. We expect that the new marker presented here (LA size divided by atrial pump function) will improve risk classification in future prospective studies.

Acknowledgments

We thank the members of the Arita Cohort Studies Unit for their valuable assistance with patient investigations, as well as Yoshiyuki Sumita, Tetsuhiro Yamano, Haruhiko Abe, and Takuya Hasegawa for obtaining excellent echocardiographic data.

Downloaded from hyper.ahajournals.org at OKAYAMA UNIV on May 2, 2011

Sources of Funding

This study was supported by a grant from the Japan Heart Foundation.

Disclosures

None.

References

1. Fleqel KM, Shipley MJ, Rose G. Risk of stroke in non-rheumatic atrial fibrillation. *Lancet*. 1987;1:526–529.
2. Lévy S, Maarek M, Coumel P, Guize L, Lekieffre J, Medvedowsky JL, Sebaoun A. Characterization of different subjects of atrial fibrillation in general practice in France: the ALFA Study. *Circulation*. 1999;99:3028–3035.
3. Wolf PA, Abbott RD, Kannel WB. Atrial fibrillation as an independent risk factor for stroke: the Framingham Study. *Stroke*. 1991;22:983–988.
4. Connolly SJ, Laupacis A, Gent M, Roberts RS, Cairns JA, Joyner C. Canadian Atrial Fibrillation Anticoagulation (CAFA) Study. *J Am Coll Cardiol*. 1991;18:349–355.
5. Gage BF, Waterman AD, Shannon W, Boechler M, Rich MW, Radford MJ. Validation of clinical classification schemes for predicting stroke: results from the National Registry of Atrial Fibrillation. *JAMA*. 2001;285:2864–2870.
6. Hohnloser SH, Pajitnev D, Pogue J, Healey JS, Pfeffer MA, Yusuf S, Connolly SJ, for the ACTIVE W Investigators. Incidence of stroke in paroxysmal versus sustained atrial fibrillation in patients taking oral anticoagulation or combined antiplatelet therapy: an ACTIVE W Substudy. *J Am Coll Cardiol*. 2007;50:2156–2161.
7. Fang MC, Go AS, Chang Y, Borowsky L, Pomernacki NK, Singer DE, for the ATRIA Study Group. Comparison of risk stratification schemes to predict thromboembolism in people with nonvalvular atrial fibrillation. *J Am Coll Cardiol*. 2008;51:810–815.
8. Albers GW, Diener HC, Frison L, Grind M, Nevinson M, Partridge S, Halperin JL, Horrow J, Olsson SB, Petersen P, Vahanian A, for the SPORTIF Executive Steering Committee for the SPORTIF V Investigators. Ximelagatran vs warfarin for stroke prevention in patients with nonvalvular atrial fibrillation: a randomized trial. *JAMA*. 2005;293:690–698.
9. Lewington S, Clarke R, Qizilbash N, Peto R, Collins R, for the Prospective Studies Collaboration. Age-specific relevance of usual blood pressure to vascular mortality: a meta-analysis of individual data for one million adults in 61 prospective studies. *Lancet*. 2002;360:1903–1913.
10. Deroubaix E, Folliguet T, Rücker-Martin C, Dinanian S, Boixel C, Validire P, Daniel P, Capderou A, Hatem SN. Moderate and chronic hemodynamic overload of sheep atria induces reversible cellular electrophysiologic abnormalities and atrial vulnerability. *J Am Coll Cardiol*. 2004;44:1918–1926.
11. Wijffels MC, Kirchhof CJ, Dorland R, Allessie MA. Atrial fibrillation begets atrial fibrillation: a study in awake chronically instrumented goats. *Circulation*. 1995;92:1954–1968.
12. Lang RM, Bierig M, Devereux RB, Flachskampf FA, Foster E, Pellikka PA, Picard MH, Roman MJ, Seward J, Shanewise JS, Solomon SD, Spencer KT, Sutton MS, Stewart WJ, for the Chamber Quantification Writing Group; American Society of Echocardiography's Guidelines and Standards Committee; European Association of Echocardiography. Recommendations for chamber quantification: a report from the American Society of Echocardiography's Guidelines and Standards Committee and the Chamber Quantification Writing Group, developed in conjunction with the European Association of Echocardiography, a branch of the European Society of Cardiology. *J Am Soc Echocardiogr*. 2005;18:1440–1463.
13. Rodrigues AC, Scannavacca MI, Caldas MA, Hotta VT, Pisani C, Sosa EA, Mathias W Jr. Left atrial function after ablation for paroxysmal atrial fibrillation. *Am J Cardiol*. 2009;103:395–398.
14. Abhayaratna WP, Seward JB, Appleton CP, Douglas PS, Oh JK, Tajik AJ, Tsang TS. Left atrial size: physiologic determinants and clinical applications. *J Am Coll Cardiol*. 2006;47:2357–2363.
15. Manning WJ, Leeman DE, Gotch PJ, Come PC. Pulsed Doppler evaluation of atrial mechanical function after electrical cardioversion of atrial fibrillation. *J Am Coll Cardiol*. 1989;13:617–623.
16. Thomas L, Boyd A, Thomas SP, Schiller NB, Ross DL. Atrial structural remodelling and restoration of atrial contraction after linear ablation for atrial fibrillation. *Eur Heart J*. 2003;24:1942–1951.
17. Nagueh SF, Sun H, Kopelen HA, Middleton KJ, Khoury DS. Hemodynamic determinants of the mitral annulus diastolic velocities by tissue Doppler. *J Am Coll Cardiol*. 2001;37:278–285.
18. Saraiva RM, Yamano T, Matsumura Y, Takasaki K, Toyono M, Agler DA, Greenberg N, Thomas JD, Shiota T. Left atrial function assessed by real-time 3-dimensional echocardiography is related to right ventricular systolic pressure in chronic mitral regurgitation. *Am Heart J*. 2009;158:309–316.
19. Thomas L, Levett K, Boyd A, Leung DY, Schiller NB, Ross DL. Changes in regional left atrial function with aging: evaluation by Doppler tissue imaging. *Eur J Echocardiogr*. 2003;4:92–100.
20. Khankirawatana B, Khankirawatana S, Peterson B, Mahrous H, Porter TR. Peak atrial systolic mitral annular velocity by Doppler tissue reliably predicts left atrial systolic function. *J Am Soc Echocardiogr*. 2004;17:353–360.
21. Barbier P, Alioto G, Guazzi MD. Left atrial function and ventricular filling in hypertensive patients with paroxysmal atrial fibrillation. *J Am Coll Cardiol*. 1994;24:165–170.
22. Anwar AM, Geleijnse ML, Soliman OI, Nemes A, ten Cate FJ. Left atrial Frank-Starling law assessed by real-time, three-dimensional echocardiographic left atrial volume changes. *Heart*. 2007;93:1393–1397.
23. Stefanadis C, Dernellis J, Toutouzas P. A clinical appraisal of left atrial function. *Eur Heart J*. 2001;22:22–36.
24. Pickering TG, Hall JE, Appel LJ, Falkner BE, Graves J, Hill MN, Jones DW, Kurtz T, Sheps SG, Roccella EJ, for the Subcommittee of Professional and Public Education of the American Heart Association Council on High Blood Pressure Research. Recommendations for blood pressure measurement in humans and experimental animals: part 1–blood pressure measurement in humans: a statement for professionals from the Subcommittee of Professional and Public Education of the American Heart Association Council on High Blood Pressure Research. *Hypertension*. 2005;45:142–161.
25. Devereux RB, Dahlof B, Levy D, Pfeffer MA. Comparison of enalapril versus nifedipine to decrease left ventricular hypertrophy in systemic hypertension (the PRESERVE Trial). *Am J Cardiol*. 1996;78:61–65.
26. Dokainish H, Zoghbi WA, Lakkis NM, Al-Bakshy F, Dhir M, Quinones MA, Nagueh SF. Optimal noninvasive assessment of left ventricular filling pressures: a comparison of tissue Doppler echocardiography and B-type natriuretic peptide in patients with pulmonary artery catheters. *Circulation*. 2004;109:2432–2439.
27. Pritchett AM, Mahoney DW, Jacobsen SJ, Rodeheffer RJ, Karon BL, Redfield MM. Diastolic dysfunction and left atrial volume: a population-based study. *J Am Coll Cardiol*. 2005;45:87–92.
28. Weber KT, Brilla CG, Janicki JS. Myocardial fibrosis: functional significance and regulatory factors. *Cardiovasc Res*. 1993;27:341–348.
29. Kai H, Kuwahara F, Tokuda K, Imaizumi T. Diastolic dysfunction in hypertensive hearts: roles of perivascular inflammation and reactive myocardial fibrosis. *Hypertens Res*. 2005;28:483–490.
30. Leite-Moreira AF, Correia-Pinto J, Gillebert TC. Afterload induced changes in myocardial relaxation: a mechanism for diastolic dysfunction. *Cardiovasc Res*. 1999;43:344–353.
31. Choisy SC, Arberry LA, Hancox JC, James AF. Increased susceptibility to atrial tachyarrhythmia in spontaneously hypertensive rat hearts. *Hypertension*. 2007;49:498–505.
32. Verdecchia P, Reboldi G, Gattobigio R, Bentivoglio M, Borgioni C, Angeli F, Carluccio E, Sardone MG, Porcellati C. Atrial fibrillation in hypertension: predictors and outcome. *Hypertension*. 2003;41:218–223.
33. Petersen P, Kastrup J, Brinch K, Godtfredsen J, Boysen G. Relation between left atrial dimension and duration of atrial fibrillation. *Am J Cardiol*. 1987;60:382–384.
34. Appleton CP, Jensen JL, Hatle LK, Oh JK. Doppler evaluation of left and right ventricular diastolic function: a technical guide for obtaining optimal flow velocity recordings. *J Am Soc Echocardiogr*. 1997;10:271–292.
35. De Boeck BW, Cramer MJ, Oh JK, van der Aa RP, Jaarsma W. Spectral pulsed tissue Doppler imaging in diastole: a tool to increase our insight in and assessment of diastolic relaxation of the left ventricle. *Am Heart J*. 2003;146:411–419.
36. Di Salvo G, Caso P, Lo Piccolo R, Fusco A, Martiniello AR, Russo MG, D'Onofrio A, Severino S, Calabró P, Pacileo G, Mininni N, Calabró R. Atrial myocardial deformation properties predict maintenance of sinus rhythm after external cardioversion of recent-onset lone atrial fibrillation: a color Doppler myocardial imaging and transthoracic and transesophageal echocardiographic study. *Circulation*. 2005;112:387–395.

Downloaded from hyper.ahajournals.org at OKAYAMA UNIV on May 2, 2011

37. Schneider C, Malisius R, Krause K, Lampe F, Bahlmann E, Boczor S, Antz M, Ernst S, Kuck KH. Strain rate imaging for functional quantification of the left atrium: atrial deformation predicts the maintenance of sinus rhythm after catheter ablation of atrial fibrillation. *Eur Heart J*. 2008;29:1397–1409.
38. Eshoo S, Boyd AC, Ross DL, Marwick TH, Thomas L. Strain rate evaluation of phasic atrial function in hypertension. *Heart*. 2009;95:1184–1191.
39. Thomas L, McKay T, Byth K, Marwick TH. Abnormalities of left atrial function after cardioversion: an atrial strain rate study. *Heart*. 2007;93:89–95.
40. Kasner M, Westermann D, Steendijk P, Gaub R, Wilkenshoff U, Weitmann K, Hoffmann W, Poller W, Schultheiss HP, Pauschinger M, Tschöpe C. Utility of Doppler echocardiography and tissue Doppler imaging in the estimation of diastolic function in heart failure with normal ejection fraction: a comparative Doppler-conductance catheterization study. *Circulation*. 2007;116:637–647.
41. Quiñones MA, Otto CM, Stoddard M, Waggoner A, Zoghbi WA, for the Doppler Quantification Task Force of the Nomenclature and Standards Committee of the American Society of Echocardiography. Recommendations for quantification of Doppler echocardiography: a report from the Doppler Quantification Task Force of the Nomenclature and Standards Committee of the American Society of Echocardiography. *J Am Soc Echocardiogr*. 2002;15:167–184.
42. Paulus WJ, Tschöpe C, Sanderson JE, Rusconi C, Flachskampf FA, Rademakers FE, Marino P, Smiseth OA, De Keulenaer G, Leite-Moreira AF, Borbély A, Edes I, Handoko ML, Heymans S, Pezzali N, Pieske B, Dickstein K, Fraser AG, Brutsaert DL. How to diagnose diastolic heart failure: a consensus statement on the diagnosis of heart failure with normal left ventricular ejection fraction by the Heart Failure and Echocardiography Associations of the European Society of Cardiology. *Eur Heart J*. 2007;28:2539–2350.
43. Rho RW, Page RL. Asymptomatic atrial fibrillation. *Prog Cardiovasc Dis*. 2005;48:79–87.
44. Hart RG, Pearce LA, Aguilar MI. Meta-analysis: antithrombotic therapy to prevent stroke in patients who have nonvalvular atrial fibrillation. *Ann Intern Med*. 2007;146:857–867.
45. Schnabel RB, Sullivan LM, Levy D, Pencina MJ, Massaro JM, D'Agostino RB Sr, Newton-Cheh C, Yamamoto JF, Magnani JW, Tadros TM, Kannel WB, Wang TJ, Ellinor PT, Wolf PA, Vasan RS, Benjamin EJ. Development of a risk score for atrial fibrillation (Framingham Heart Study): a community-based cohort study. *Lancet*. 2009;373:739–745.

Downloaded from hyper.ahajournals.org at OKAYAMA UNIV on May 2, 2011